

A Two-way Stratosphere–Troposphere Coupling of Submonthly Zonal-Mean Circulations in the Arctic

LI Xiaofeng¹ (李晓峰), LI Jianping^{*1} (李建平), and Xiangdong ZHANG²

¹*State Key Laboratory of Numerical Modeling for Atmospheric Sciences and Geophysical Fluid Dynamics, Institute of Atmospheric Physics, Chinese Academy of Sciences, Beijing 100029*

²*International Arctic Research Center, University of Alaska Fairbanks, Fairbanks, Alaska 99775, United States*

(Received 27 August 2012; revised 3 December 2012; accepted 25 January 2013)

ABSTRACT

This paper examines the dominant submonthly variability of zonally symmetrical atmospheric circulation in the Northern Hemisphere (NH) winter within the context of the Northern Annular Mode (NAM), with particular emphasis on interactive stratosphere–troposphere processes. The submonthly variability is identified and measured using a daily NAM index, which concentrates primarily on zonally symmetrical circulation. A schematic lifecycle of submonthly variability is developed that reveals a two-way coupling process between the stratosphere and troposphere in the NH polar region. Specifically, anomalous tropospheric zonal winds in the Atlantic and Pacific sectors of the Arctic propagate upwards to the low stratosphere, disturbing the polar vortex, and resulting in an anomalous stratospheric geopotential height (HGT) that subsequently propagates down into the troposphere and changes the sign of the surface circulations.

From the standpoint of planetary-scale wave activities, a feedback loop is also evident when the anomalous planetary-scale waves (with wavenumbers 2 and 3) propagate upwards, which disturbs the anomalous zonally symmetrical flow in the low stratosphere, and induces the anomalous HGT to move poleward in the low stratosphere, and then propagates down into the troposphere. This increases the energy of waves at wavenumbers 2 and 3 in the low troposphere in middle latitudes by enhancing the land–sea contrast of the anomalous HGT field. Thus, this study supports the viewpoint that the downward propagation of stratospheric NAM signals may not originate in the stratosphere.

Key words: zonal-mean circulation, stratosphere–troposphere interaction, polar vortex, Northern Hemisphere Annular Mode

Citation: Li, X. F., J. P. Li, and X. D. Zhang, 2013: A two-way stratosphere–troposphere coupling of submonthly zonal-mean circulations in the Arctic. *Adv. Atmos. Sci.*, **30**(6), 1771–1785, doi: 10.1007/s00376-013-2210-4.

1. Introduction

The Northern Hemisphere Annular Mode (NAM), or Arctic Oscillation (AO), is a fundamental hemispheric-scale leading mode that explains a large proportion of the variance in the Northern Hemisphere (NH) atmospheric circulation (Thompson and Wallace, 1998, 2000; Li and Wang, 2003). Although the NAM is conventionally defined using monthly sea level pressure (SLP) data, it has a broader spectrum of variability, ranging from daily variations to synoptic

weather patterns (the intrinsic timescale of the NAM). Its aggregated effect from the short timescales explains the variability of the NAM at monthly, and longer, timescales. The NAM has a strong positive correlation with integrative synoptic activity (Zhang et al., 2004), and is also strongly linked to the stratospheric polar vortex (Baldwin and Dunkerton, 1999, 2001; Baldwin et al., 2003b), far above sea level. An understanding of these connections and linkages may help to identify the role played by the NAM in steering daily to interannual variations in atmospheric circulation patterns.

* Corresponding author: LI Jianping, ljp@lasg.iap.ac.cn

The variations in the intensity of the stratospheric polar vortex, and the associated downward-propagating geopotential height (HGT) anomalies, have a strong influence on NAM amplitude (Baldwin and Dunkerton, 1999; Black et al., 2009). This downward propagation of the NAM signal from the stratosphere, on intraseasonal timescales of around three months, provides a more efficient extended-range forecast of tropospheric circulation than does the tropospheric signal itself (Baldwin et al., 2003a, b). However, it remains unclear how synoptic-scale stratosphere–troposphere interactions are related to the variability associated with the NAM. Studying the nature of these interactions over the synoptic timescale may improve our understanding of the internal dynamic processes of the stratosphere–troposphere coupling.

In this paper, we aim to develop a better understanding of the processes outlined above. Given the nature of the Earth's atmospheric dynamics, a prominent feature of extratropical atmospheric circulation is zonal symmetry in both its climatology and variability, represented by the NAM. According to the most recent perspective on the zonally symmetrical modes of variability in NH circulation, the NAM represents the reemergence of the Zonal Index Paradigm (Thompson et al., 2003; Li and Wang, 2003), which can be traced back to Rossby's research in the late 1930s (Rossby, 1939).

Here, a zonal-mean approach is used to focus on this zonally symmetrical feature of atmospheric circulation. We use a modified zonal index (Li and Wang, 2003), based on daily data, rather than the conventionally defined NAM index (NAMI) that is derived from monthly data. This modified index covers variability spectra from synoptic to hemispheric scales, and performs well in capturing the NAM patterns in the SLP field, although it expresses a more symmetrical ring structure, and it can be used as an alternative NAMI (Li and Wang, 2003). Angell (2006), Gao and Washington (2010) and Lee et al. (2012) pointed out that this simple NAMI has a more symmetric correlation with SLP than does the first principal component (PC1) of Thompson and Wallace (1998, 2000). As this NAMI is simply defined as the standardized difference in zonal-averaged SLP between the two most negatively correlated zonal belts in middle and high latitudes [i.e. the mid- and high-latitude Annular Belt of Actions (ABAs)] (Li and Wang, 2003), it emphasizes the connection between these regions. Based on this NAMI, we first identify submonthly fluctuations in the zonal-mean atmospheric circulation, then examine associated stratosphere–troposphere interactions over the northern polar region, and finally inves-

tigate planetary-scale wave activity during these interactions.

2. Data and methodology

2.1 Data

The central dataset used in this study is the daily average values from the National Centers for Environmental Prediction–National Center for Atmospheric Research (NCEP–NCAR Reanalysis from 1 January 1948 to 31 December 2006, as obtained from the National Oceanic and Atmospheric Climate Diagnostics Center (Kalnay et al., 1996). An empirical orthogonal function/principal component (EOF/PC) NAM index from the National Oceanic and Atmospheric Administration (NOAA) Climate Prediction Center (CPC), CPC-NAMI, is also used here for comparison with the NAMI. For convenience, we excluded data for 29 February in leap years, which does not affect the final results. In this study, the winter season refers to the period from November to March, and is referred to as NDJFM.

2.2 Daily NAM Index

The NAMI proposed by Li and Wang (2003) is used here, although with daily resolution (Li and Li, 2009, 2011). This NAMI, which is based on the zonal index paradigm, represents a measure of the hemispheric-wide fluctuations in air mass between two ABAs at middle and high latitudes, centered near 35°N and 65°N, respectively, and is defined as follows:

$$I_{\text{NAM}} = \hat{P}_{35N} - \hat{P}_{65N}, \quad (1)$$

where P is the daily zonally-averaged SLP, and \hat{P}_{35N} and \hat{P}_{65N} are the normalized values of P at latitudes of 35°N and 65°N, respectively. The zonally symmetrical SLP generally shows a negative correlation between these two latitudes in the NH subtropics (Li and Wang, 2003). The normalization of \hat{P} for a given year n , and day m , is:

$$\hat{P}_{m,n} = \frac{P'_{m,n}}{S_P}, \quad (2)$$

where $P'_{m,n}$ is the daily pressure anomaly of $P_{m,n}$, a departure from the 1958–2000 base period, and S_P is the total standard deviation of the daily anomaly $P'_{m,n}$ time series, i.e.

$$S_P = \sqrt{\frac{1}{365 \times 43} \sum_{i=1958}^{2000} \sum_{j=1}^{365} P'_{j,i}^2}. \quad (3)$$

The spatial structure of the NH SLP field, represented by the daily NAMI, is a zonally symmetrical north-south seesaw pattern in the extratropics. As shown

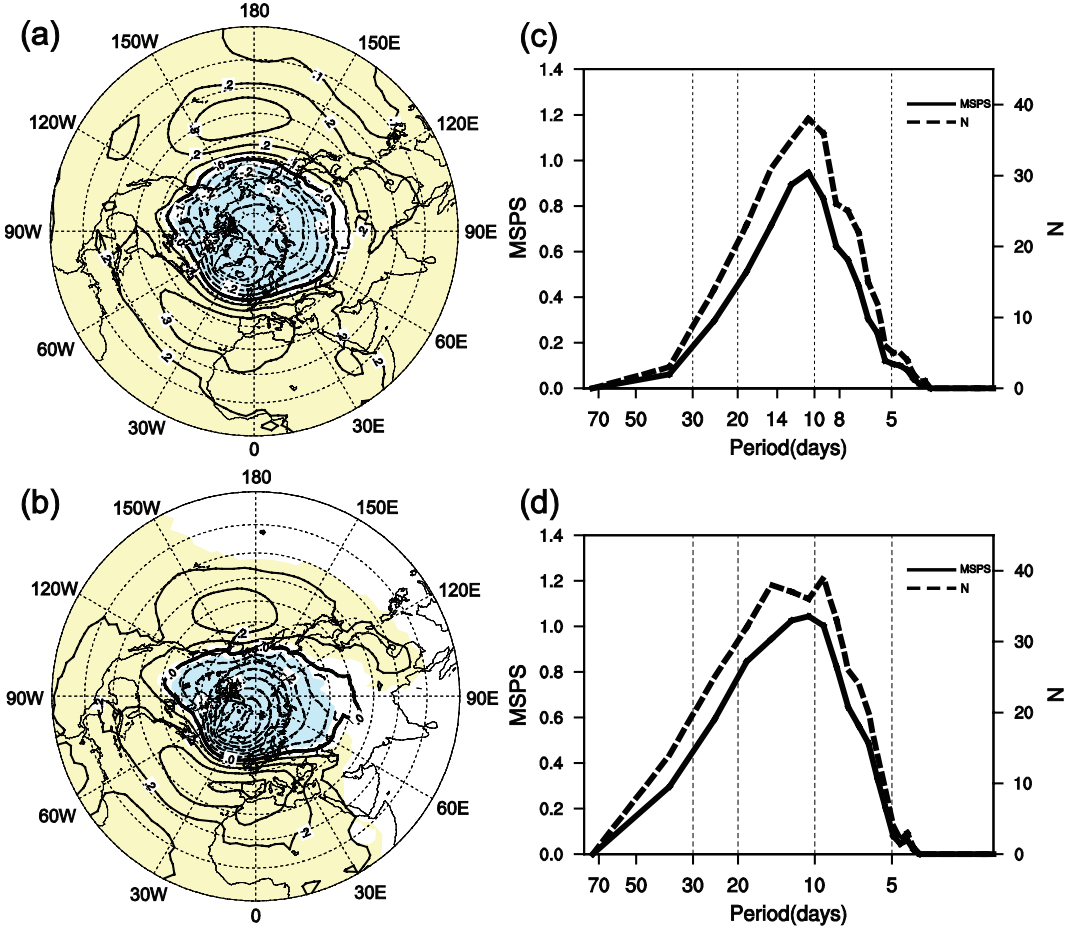


Fig. 1. Correlation maps of daily sea level pressure (SLP) anomalies in the NH (1 Jan 1950–31 Dec 2005) using (a) the NAMI and (b) the CPC-NAMI (from <ftp://ftp.cpc.ncep.noaa.gov/cwlinks/>). Also shown are the mean standard power spectrum (MSPS, solid line) and N (dashed line) for (c) the NAMI and (d) the CPC-NAMI for 58 winters (1948–2004). The contour interval is 0.1. Shading indicates statistical significance at the 99.9% level, and the efficient freedom of degrees is estimated in each grid (Davis, 1976). The latitude lines are at 10° intervals, starting with the equator at the edges.

in Fig. 1a, the daily NAMI is positively correlated with SLP anomalies over subtropical and mid-latitude regions, and exhibits a strong negative correlation with SLP anomalies over high latitudes and the polar region, indicating an out-of-phase relationship between SLP anomalies in high- and mid-latitude zones. In the Pacific and Atlantic sectors, two obvious regional centers exist in the subtropical zones. A comparison between the pattern in the SLP field captured by the CPC-NAMI (Fig. 1b), and the pattern captured by the NAMI (Fig. 1a), reveals similar basic features, but the NAMI pattern represents a more zonally symmetrical feature.

2.3 Submonthly timescales of the daily NAMI in the winter season

Although the NAMI has a red tendency (i.e. low frequencies/longer periods tend to be associated with

an intense power spectrum), year-by-year spectral analysis of the winter season data (not shown) indicates the presence of a statistically significant periodicity. Statistically significant periods distribute mainly in submonthly periods of 5–30 days, centering around 10 days. Below, we calculate two variables to clarify these features.

To determine which frequency or period band has the highest probability of being statistically significant during the 58 winters considered in the present study, the number of significant years (N) in an individual frequency range from $f = 0$ to $f = f_{Ny}$ (the Nyquist frequency) during the winters of 1948–2005 was calculated (Li and Li, 2009, 2011; Sun and Li, 2012) as follows:

$$N = \sum_{i=1948}^{2005} k_i, \quad k_i = \begin{cases} 1, & S \geq S_{95} \\ 0, & S < S_{95} \end{cases} . \quad (4)$$

Here, k is the number of significant spectral peaks in one year, i represents the year from 1948 to 2005, S is the power spectrum in winter and S_{95} is the 95% upper confidence level.

The power spectrum in submonthly bands appears to more readily attain the upper red noise confidence level than do other bands, i.e. significant spectra relative to the upper confidence level are more intense at submonthly timescales than in other bands. The mean standard power spectrum (MSPS) is designed to indicate this relative intensity of evident spectra against the red background (Li and Li, 2009; Sun and Li, 2012). The MSPS is the average of the Standard Power Spectrum (SPS) in winters from 1948 to 2005:

$$\overline{R^*} = \frac{1}{58} \sum_{i=1948}^{2005} (R^*)_i, \quad (5)$$

where R^* is the SPS, defined as:

$$R^* = S^*/S_{95}, \quad (6)$$

and where S^* is the power spectrum, which is assigned a value of zero when not statistically significant:

$$S^* = \begin{cases} S, & S \geq S_{95} \\ 0, & S < S_{95} \end{cases}. \quad (7)$$

In Figs. 1c and d, N and MSPS of both NAMI and CPC-NAMI are largest for submonthly periods of between 5 and 30 days, with peaks centered near 10 days. This result indicates that not only do the submonthly period bands centered near 10 days have a higher probability of being statistically significant during the past 58 winters, but that the spectra in this band are more intense relative to the upper confidence level. Therefore, the submonthly variability centered approximately at 10 days dominates the daily temporal evolution of zonally symmetrical circulations in the context of the NAM. This is consistent with the results by Feldstein (2000) that the e-folding timescale of the NAM in the troposphere is about 10 days. Based on the above analysis, we herein focus on submonthly variability.

2.4 Composite analysis of submonthly NAM events

To capture the essential features of the submonthly fluctuations in NH zonal-mean circulation associated with the NAMI, the submonthly NAM lifecycles were isolated and divided into 16 equal time intervals and denoted by 17 time points using linear interpolation, for composite analysis. A submonthly NAM lifecycle consists of the complete positive phase of a cycle, followed by a complete negative phase, each of which has

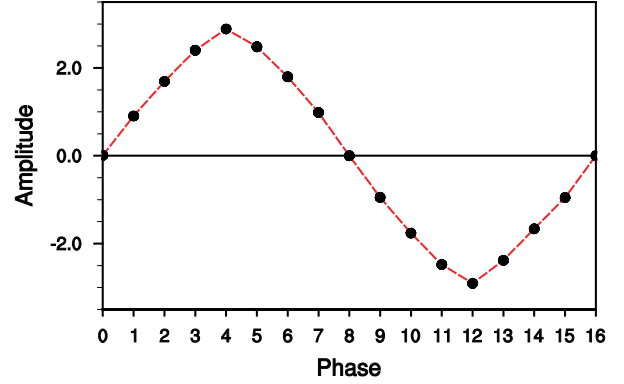


Fig. 2. Composite evolution of the submonthly NAMI lifecycle. The ordinate represents the composite NAMI index, and the abscissa is the time phase of the composite NAM event.

a peak amplitude greater than two standard deviations from the mean of the NAMI during the base period (1958–2000), starting and ending at the nearest day with zero amplitude. The Lanczos bandpass digital filter (Duchon, 1979) with 601 weights was used to isolate the submonthly variability with a period of 5–30 days. Variability with a period of <5 days was discarded to avoid disturbance by high-frequency noise. After time filtering, the data in the first and last years were removed. The submonthly NAM events were selected in winters from 1949 to 2004, but were discarded if they extended into non-winter months. We selected 142 positive and 119 negative events from the 56-year span, representing an average of 2–3 positive and negative events each winter. Figure 2 shows a complete submonthly NAM lifecycle, with 17 phases, which represents a composite NAM event starting at phase 0, reaching the highest positive amplitude at phase 4, changing from positive to negative amplitude at phase 8, reaching the strongest negative amplitude at phase 12, and ending at phase 16. At each phase of the submonthly NAM lifecycle, the submonthly circulation anomalies are composited to represent the temporal and spatial evolution of individual cases.

3. Stratosphere–troposphere coupling of the submonthly zonal-mean circulation in the Northern Hemisphere

3.1 Overall features of the lifecycle of submonthly NAM events

Considering the zonally symmetrical and quasi-barotropic characteristics of the NAM (Thompson and Wallace, 1998, 2000), the basic features of submonthly NAM events are well represented by the evolution of zonal average vertical atmospheric circulations. The

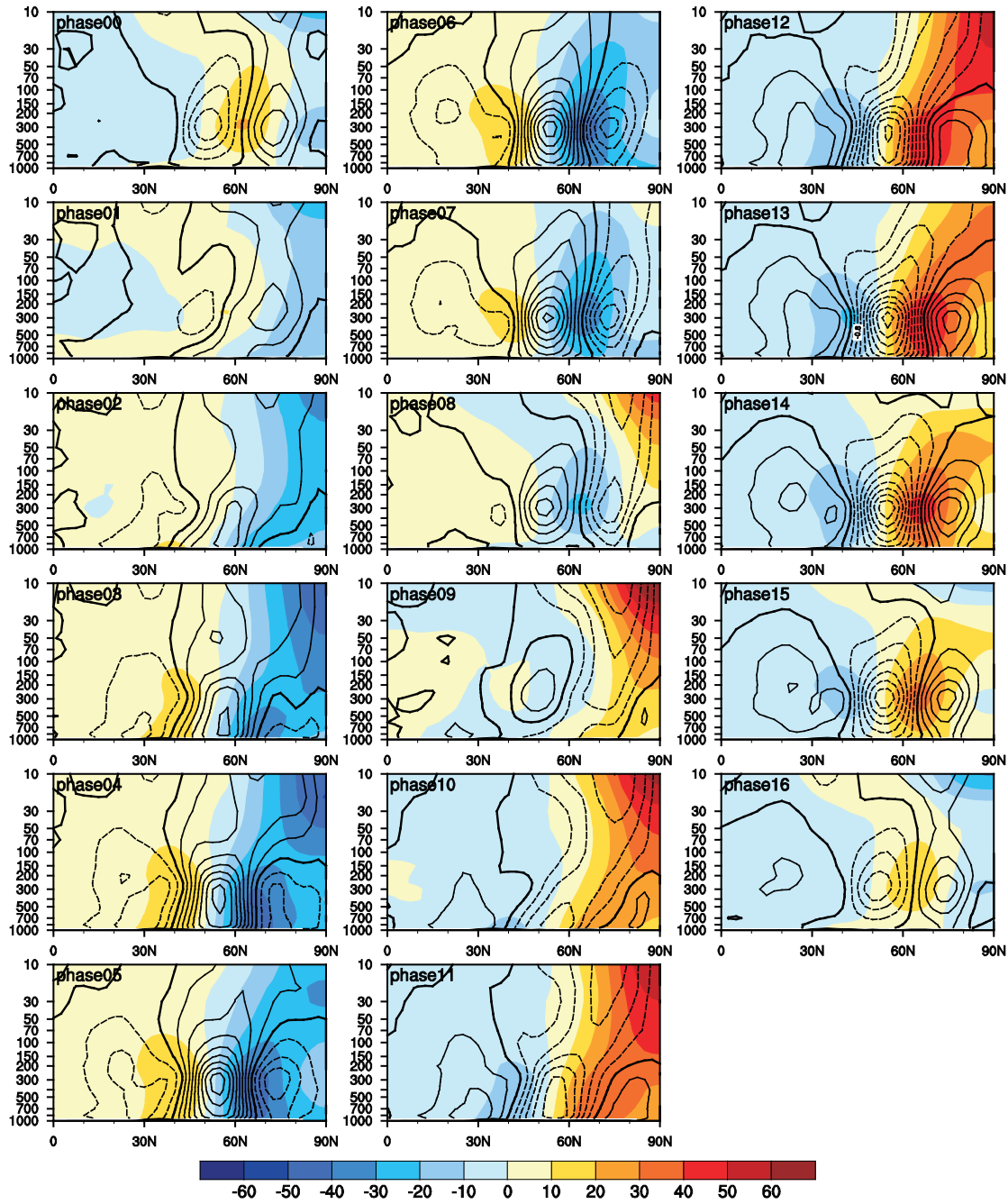


Fig. 3. Composite evolution of zonal-mean submonthly anomalies of HGT (color shading; units: gpm) and zonal wind (contour interval: 0.2 m s^{-1} ; the zero contour is bold) from phase 0 to 16 during the lifecycles of submonthly NAM events in NDJFM.

variation of the submonthly NAM lifecycle indicates the evolution of a zonally symmetrical north–south mass seesaw between middle and high latitudes in the NH extratropics (Fig. 3). During the developing stage (phases 1–3 in Fig. 3), at high latitudes centered near 65°N the negative HGT anomalies intensify from the near-surface up to the tropopause, while similarly, at middle latitudes centered around 40°N the positive

HGT anomalies intensify from the near-surface up to the tropopause. This indicates that the anomalous atmospheric mass is dissipated at high latitudes, but accumulates at middle latitudes, resulting in an equivalent barotropic atmospheric mass seesaw between the middle and high latitudes, which is separated by a narrow transition zone at around 50°N . This north–south mass seesaw reaches a maximum in phase 4, when the

atmospheric mass attains a maximum at middle latitudes south of 50°N , and reaches a minimum at middle latitudes north of 50°N , as measured by the anomalous column HGT. The seesaw then weakens between phases 5 and 8, characterized by a decrease in positive HGT at middle latitudes, and an increase in negative HGT at high latitudes. During the subsequent negative phases of the NAM lifecycle (phases 9–16), the seesaw reverses: the mass accumulates at high latitudes, but dissipates at middle latitudes.

Anomalous zonally-averaged zonal wind also varies with the zonal-mean HGT field; thus, the geostrophic equilibrium between them is maintained at middle to high latitudes. Three symmetrical zonal wind belts occur during the positive (negative) phase of the NAM lifecycle, including an anomalous easterly (westerly) wind at low latitudes centered near 30°N , an anomalous westerly (easterly) wind at middle latitudes centered near 55°N , and an anomalous easterly (westerly) wind in the polar region centered near 70°N . The zonal wind anomalies in these three belts are enhanced during phases 0–4 (contours in Fig. 3), attain a maximum during phase 5 (with the extreme zonal wind centers rising up from the near-surface to the tropopause), decrease during phases 6–8, shift and change to a negative phase during phases 9–13, attain a minimum at phase 13 (when the extreme zonal wind centers rise up from the near-surface to the tropopause), and finally decrease during phases 14–16.

3.2 Two-way stratosphere–troposphere coupling in the polar region

In the polar regions (north of 70°N), a two-way interaction process between the tropospheric zonal wind and stratospheric geopotential height anomaly is observed during the NAM lifecycle (Fig. 3). The easterly (westerly) wind anomalies first emerge at the near-surface close to the North Pole during phase 1 (7), are subsequently strengthened near 75°N , and extend upwards. These easterly (westerly) wind anomalies penetrate the tropopause and reach 10 hPa during phase 6 (15); at the same time, positive (negative) HGT anomalies emerge at 10 hPa and subsequently propagate downward to the troposphere. Consequently, a feedback loop develops, with the troposphere influencing the stratosphere via upward zonal wind anomalies, and the stratosphere influencing the troposphere via the downward propagation of geopotential anomalies.

This two-way interaction process is illustrated in Fig. 4a. In the NH polar region, the positive (negative) HGT anomalies always propagate downward from the stratosphere to the troposphere; consequently, the easterly (westerly) wind anomalies propagate upwards from the near-surface to the stratosphere. In this two-

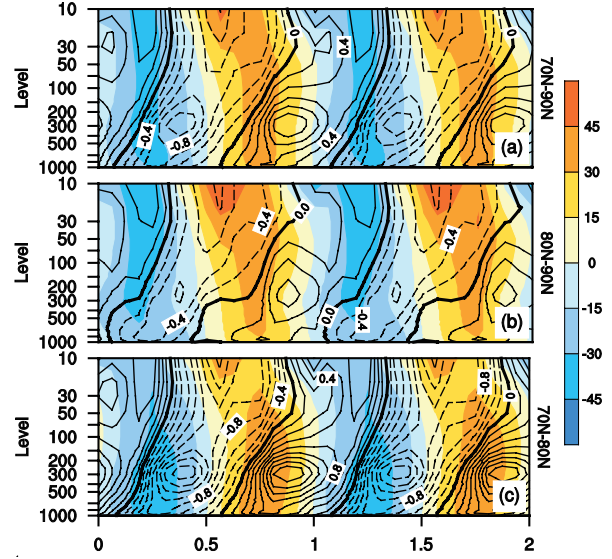


Fig. 4. Composite evolution of zonal-mean HGT anomalies (color shading; units: gpm) and zonal wind anomalies (contour interval: 0.2 m s^{-1}) as a function of the pressure level and lifecycle phase of submonthly NAM events in NDJFM. The data are the average values for (a) 70° – 90°N , (b) 80° – 90°N and (c) 70° – 80°N . On the abscissa, the number “1” (“2”) indicates one (two) complete lifecycle(s) of NAMI events, while “0.5” and “1.5” indicate the end of the positive phase and the start of the negative phase, respectively.

way coupling process, the descent of stratospheric positive (negative) HGT anomalies seems to be triggered by the ascent of tropospheric easterly (westerly) wind anomalies. A comparison of Figs. 4b and c reveals that the downward propagation of HGT anomalies near the North Pole (80° – 90°N) is more intense than that in the region south of the North Pole (70° – 80°N), while the upward propagation of zonal wind anomalies occurs in the opposite manner, i.e. the upward-propagating zonal wind anomalies are centered mainly in the region south of the North Pole (70° – 80°N), whereas downward-propagating HGT anomalies are centered mainly near the North Pole (80° – 90°N).

Previous studies (Baldwin and Dunkerton, 1999; Cai and Ren, 2006) emphasize the downward propagation of symmetrical HGT and zonal wind anomalies over intraseasonal timescales of around three months, in the stratosphere–troposphere coupling associated with the NAM. Here, however, a two-way coupling process was observed within the submonthly NAM variability, which implies that the interaction between the zonal-mean stratospheric and tropospheric circulations over short timescales is different to that over intraseasonal timescales, i.e. the stratosphere–troposphere coupling process is dependent on timescale. In the following section, we ex-

amine in detail the spatial structure of this two-way stratosphere–troposphere coupling process.

4. Spatial structure of the two-way stratosphere–troposphere coupling

4.1 Spatial structure of the submonthly NAM events in the low troposphere

To determine the spatial structure of this two-way vertical interaction between the stratosphere and troposphere within the framework of NAM variability, we first consider the variability of zonal winds in the low

troposphere (850 hPa).

Although the anomalous atmospheric circulations associated with the NAM are essentially homogeneous along the latitudinal circle, and indicate an obvious zonally symmetrical spatial structure, two intensified centers occur in the Pacific and Atlantic sectors, along with a weak center over Eurasia. The Pacific sector contains a pair of anomalous HGT centers (Fig. 5), with a southern positive (negative) center near (35°N , 170°W), and a northern negative (positive) center near (65°N , 150°W). Correspondingly, three zonal wind anomaly centers, arranged in a sandwich structure,

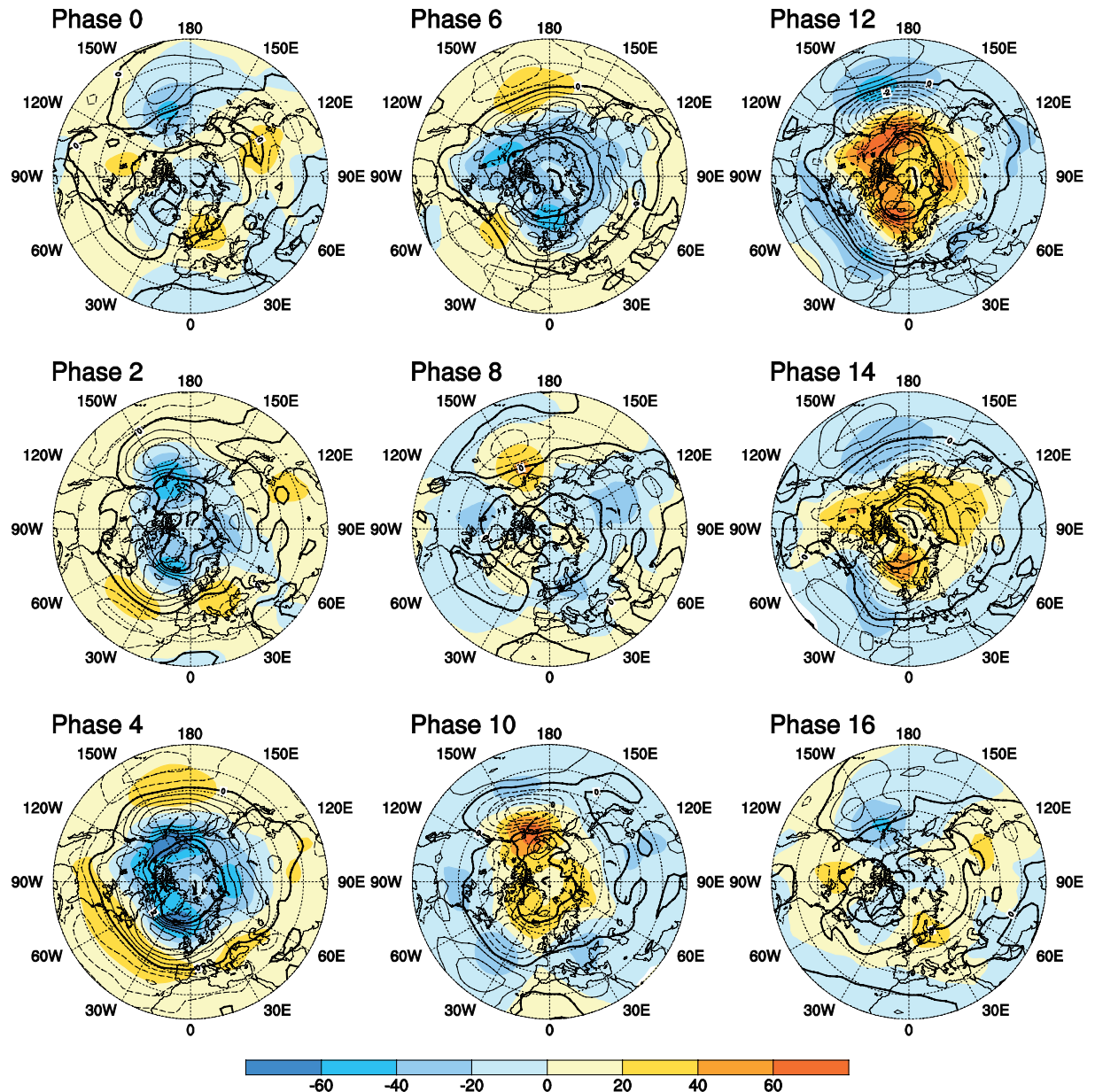


Fig. 5. Submonthly HGT anomaly at 1000 hPa (color shading; units: gpm) with the zonal wind anomaly at 850 hPa (contour interval: 1 m s^{-1}) for the lifecycle (phases: 0, 2, 4, 6, 8 and 10) of submonthly NAM events. The outermost circle in each panel represents a latitude of 20°N .

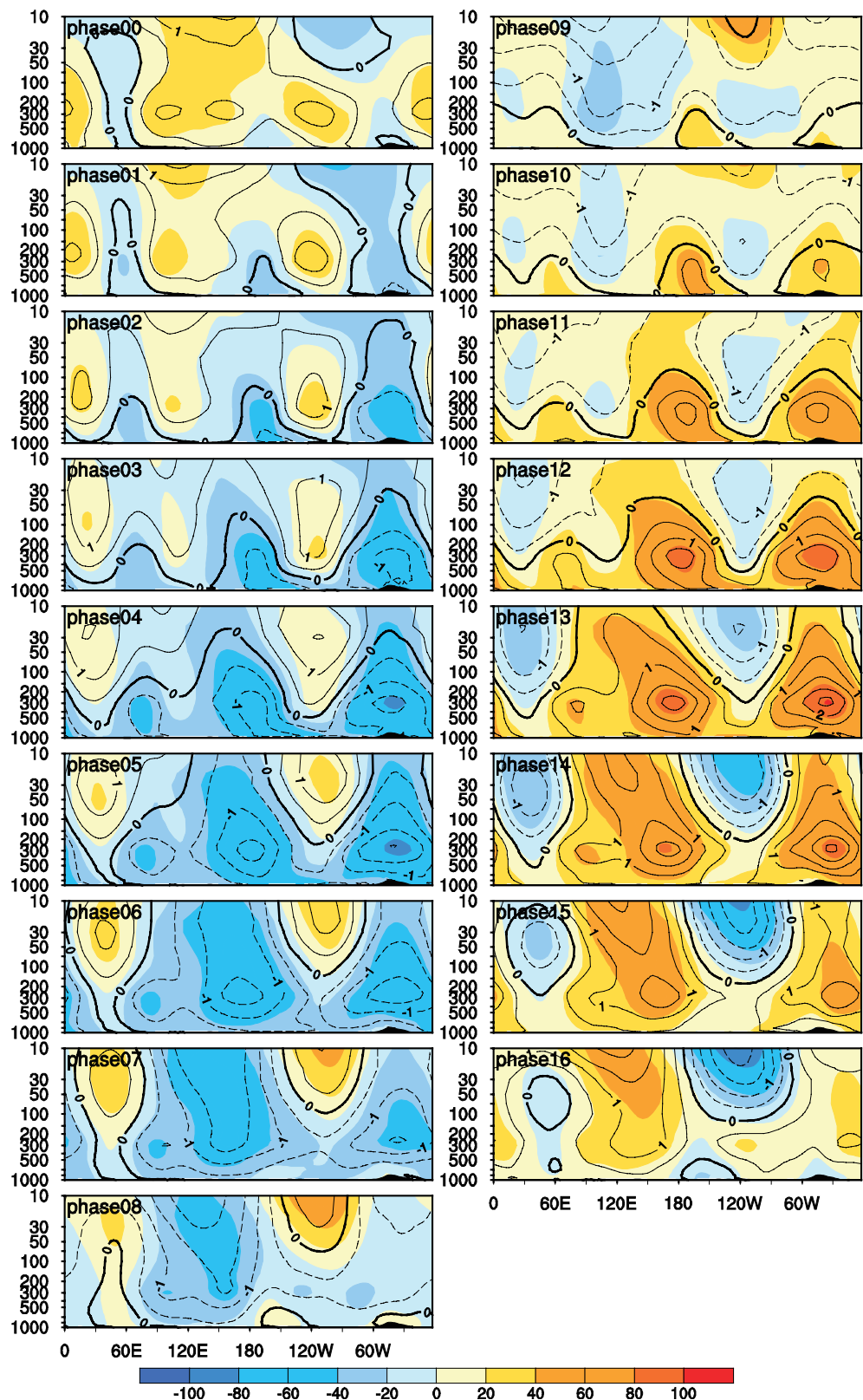


Fig. 6. Variation in the average mean HGT anomaly (shading; units: gpm) at high latitudes (60° – 70° N) and the average mean zonal wind anomaly (contour interval: 0.5 m s^{-1} ; the zero contour is bold) in the polar region (north of 70° N) as a function of pressure level and longitude associated with the lifecycle phase of submonthly NAM events.

occur between the anomalous height centers, with a central westerly (easterly) center located near (55°N , 160°W), a southern easterly (westerly) center located near (25°N , 170°W), and a northern easterly (westerly) center near (75°N , 170°W). Similarly, a pair of height anomaly centers is located over the Atlantic sector, with a southern positive (negative) center near (40°N , 60°W), and a northern negative (positive) center near (65°N , 20°W). They are also accompanied by three zonal wind anomaly centers in a sandwich structure, comprising a central westerly (easterly) center located near (55°N , 30°W), a southern easterly (westerly) center near (30°N , 20°W), and a northern easterly (westerly) center near (70°N , 10°W). The third regional center, located at high latitudes over the eastern Eurasian continent near (65°N , 90°E), with a negative (positive) height anomaly, is much weaker than the features in the Pacific and Atlantic sectors. This center is accompanied by an anomalous easterly (westerly) center near (75°N , 90°E), and an anomalous westerly (easterly) center near (55°N , 70°E), located north and south of the HGT anomaly center, respectively. So, the circulations associated with the NAM show a quasi-zonally symmetrical structure, with intense area centers above, and these intense area centers are a pair of north-south height anomaly centers accompanied by a sandwich zonal wind anomaly struc-

ture located in both the Atlantic and Pacific sectors.

4.2 Upward propagation of zonal winds in the polar region of the Pacific and Atlantic sectors

To show the longitudinal structure of the upward propagation of the zonal wind anomalies in the polar regions during the coupling process, the average value of anomalous zonal wind for $70^{\circ}\text{--}90^{\circ}\text{N}$ is shown in Fig. 6, phase by phase. In the positive (negative) phase of the NAM events, easterlies (westerlies) emerge in the near-surface of the polar region of the Pacific sector ($70^{\circ}\text{--}90^{\circ}\text{N}$, $140^{\circ}\text{E}\text{--}160^{\circ}\text{W}$) and Atlantic sector ($70^{\circ}\text{--}90^{\circ}\text{N}$, $30^{\circ}\text{W}\text{--}0^{\circ}$), then propagate upward, penetrating the tropopause and the low stratosphere, clearly indicating the upward propagation of zonal wind anomalies in these regions. To maintain the geostrophic equilibrium between the zonal wind and the HGT field, the anomalous negative (positive) HGT in the high latitudes ($60^{\circ}\text{--}70^{\circ}\text{N}$) of the Pacific and Atlantic sectors also shows upward propagation features (Fig. 6). The area average of anomalous zonal wind and HGT in the above regions (Fig. 7) shows the upward propagation features more clearly. In the polar regions of the troposphere, areas with strong upward propagation of zonal wind anomalies are mainly located in the Pacific and Atlantic sectors, where the northern belts of the

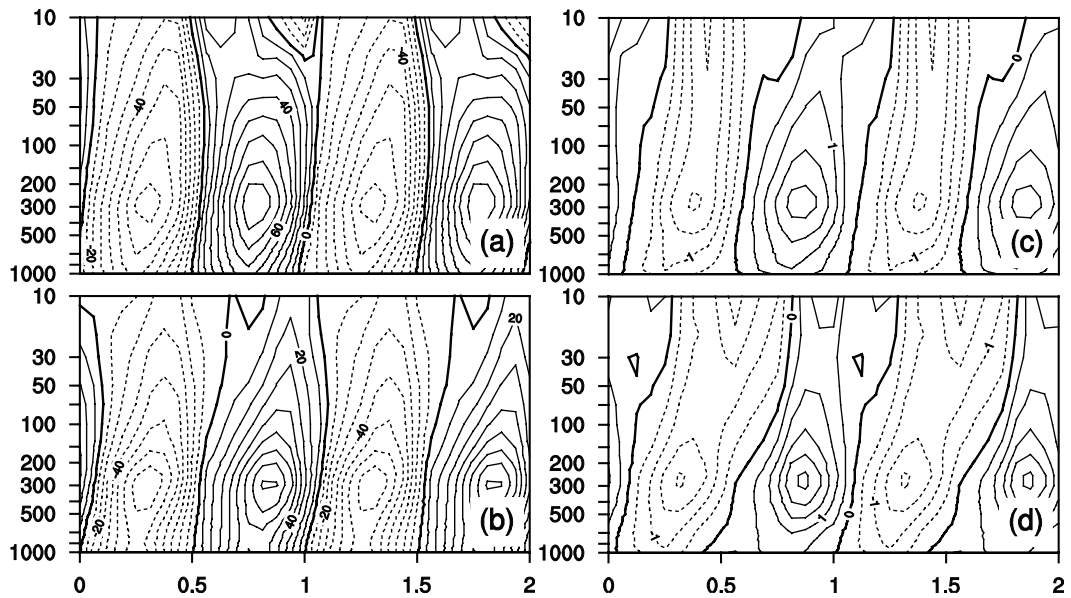


Fig. 7. Circulation anomalies as a function of the pressure level and lifecycle phase of submonthly NAM events, showing HGT anomalies (units: gpm) for (a) the Atlantic sector ($60^{\circ}\text{--}70^{\circ}\text{N}$, $30^{\circ}\text{W}\text{--}0^{\circ}$) and (b) the Pacific sector ($60^{\circ}\text{--}70^{\circ}\text{N}$, $150^{\circ}\text{E}\text{--}150^{\circ}\text{W}$), and zonal wind anomalies (units: m s^{-1}) for (c) the polar region of the Atlantic sector ($70^{\circ}\text{--}90^{\circ}\text{N}$, $30^{\circ}\text{W}\text{--}0^{\circ}$) and (d) the polar region of the Pacific sector ($70^{\circ}\text{--}90^{\circ}\text{N}$, $140^{\circ}\text{E}\text{--}160^{\circ}\text{W}$). On the abscissa, the number “1” (“2”) indicates one (two) complete lifecycle(s) of NAM events, while “0.5” and “1.5” indicate the end of the positive phase and the start of the negative phase, respectively.

sandwich zonal wind anomalies are also located.

4.3 Feedback of the polar vortex and related mass redistribution in the low stratosphere

During the lifecycle of NAM events, the polar vortex is shrinking or relaxing phase by phase. For example, the left-hand panel in Fig. 8 shows that the isoheight contour of 19 455 gpm at 50 hPa contracts during phases 4–12, indicating an increase in HGT in the polar region and a weakening of the polar vortex. In the adjoining phases, during phases 12–14 (right-hand panel in Fig. 8), the isoheight line of 19 455 m at 50 hPa expands, indicating strengthening of the polar vortex and a decrease in HGT within the polar region in the low stratosphere.

The shrinking or relaxing of the polar vortex is mainly attributed to the upward propagation of the zonal wind anomalies from the troposphere. The upward propagation of the tropospheric zonal wind anomalies mainly occurs in the polar region of the Atlantic and Pacific, as mentioned above, and acts as an external forcing to the stratospheric vortex. After the anomalous easterlies (westerlies) in these two sectors propagate to the low stratosphere at 50 hPa and become dominant during phases 4–5 (12–13), the Arctic circumpolar westerly in the low stratosphere is suppressed (instigated), and the stratospheric HGT is consequently increased (decreased) to maintain the geostrophic equilibrium, causing the polar vortex to weaken (strengthen) (Fig. 9).

The variation of the Polar vortex indicates a mass redistribution in the low stratosphere; specifically, the

poleward propagation of mass anomaly over the North American and West Eurasian sectors above the lower stratosphere results in the downward propagation of the HGT anomaly into the troposphere. As shown in Fig. 9, when the Polar vortex weakens (strengthens), the anomalous stratospheric positive (negative) HGT over the North American and West Eurasian sectors flows into the polar region from high latitudes, indicating the poleward propagation of the mass anomaly. Accompanying the accumulation of anomalous mass near the North Pole, the HGT anomaly subsequently propagates downward to the low stratosphere (as observed in Fig. 4), forming the two-way coupling process. This suggests that the polar vortex plays an important role in linking the interaction process between the zonal mean circulations of the troposphere and those of the stratosphere in polar regions of the NH.

From the above we can see the circulation in the troposphere affects the stratosphere via the upward propagation of a zonal wind anomaly in the polar region of the Atlantic and Pacific sectors, from the near-surface to the stratosphere, which induces a disturbance of the polar vortex; subsequently, the atmospheric mass in the low stratosphere is redistributed by the stratospheric HGT anomaly that flows into the polar region from the North American and European sectors. As part of a feedback loop, the HGT anomaly in the low stratosphere over the polar region subsequently propagates downward to the low troposphere, forming a two-way coupling process between the stratosphere and troposphere over the polar regions.

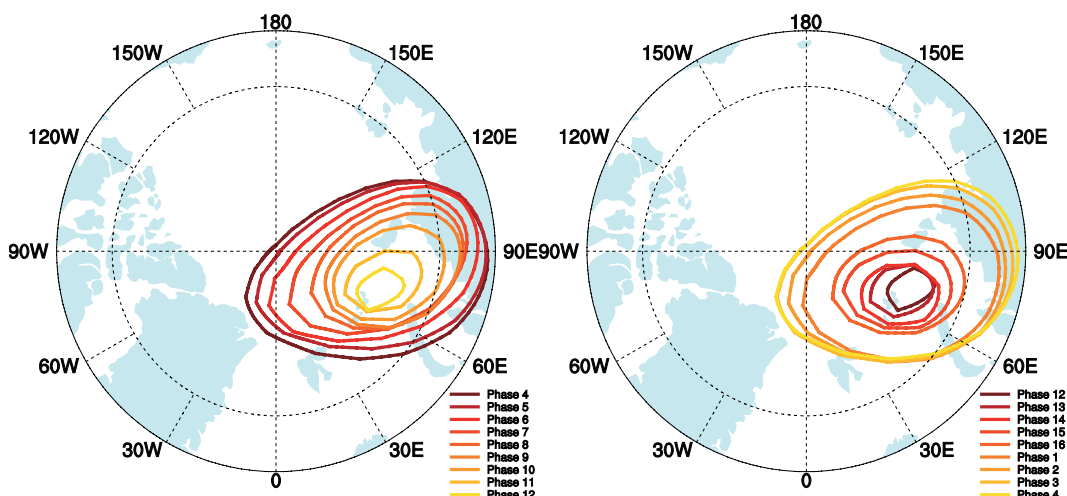


Fig. 8. Variation in the polar vortex (represented by isoheight lines of 19 455 gpm) at 50 hPa during phases 4 to 12 (left-hand panel) and phases 12 to 4 (right-hand panel) of the lifecycle of the NAM mass seesaw.

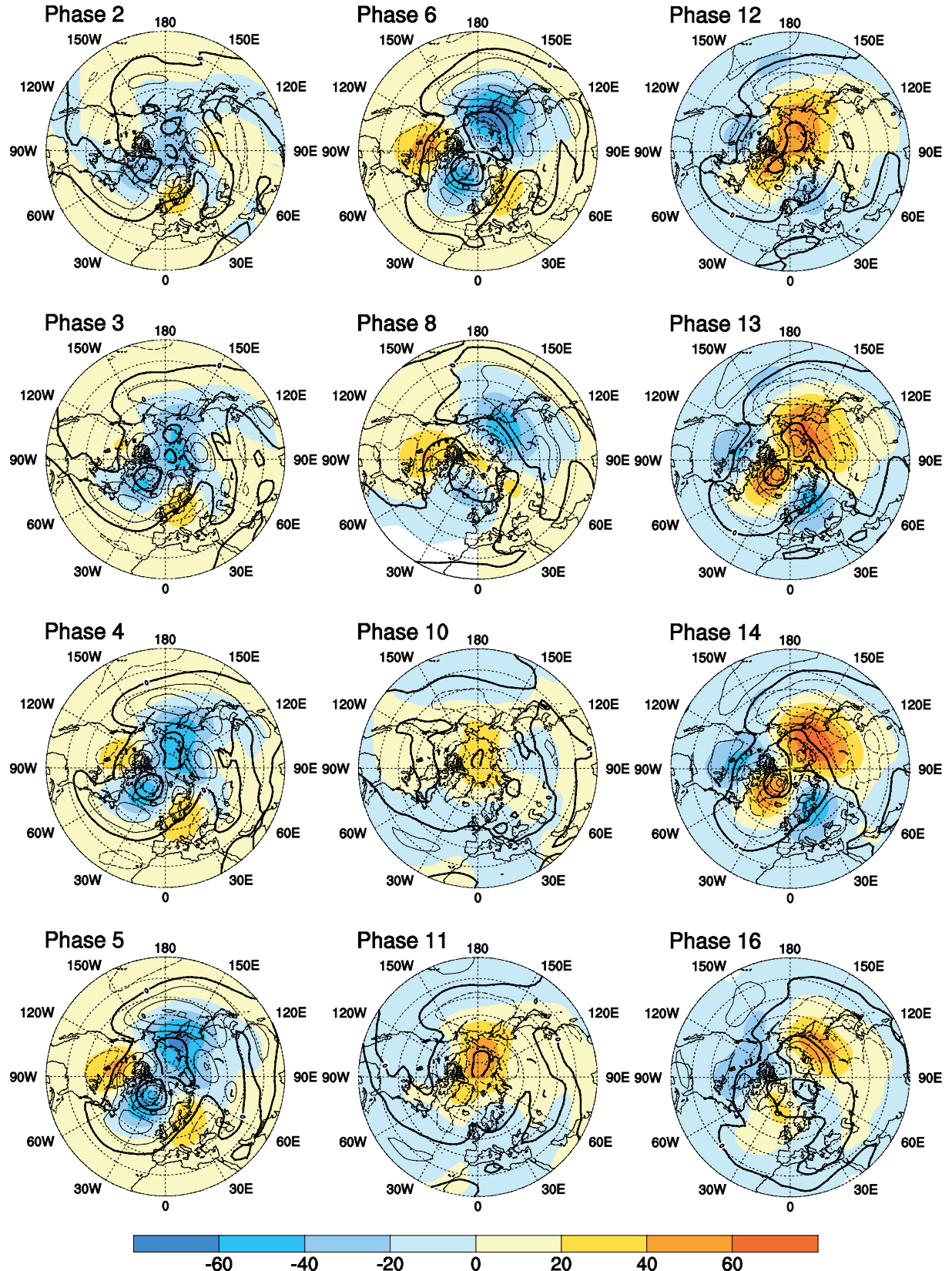


Fig. 9. Submonthly HGT (color shading; units: gpm) and zonal wind anomalies (contour interval: 1 m s^{-1}) at 50 hPa for the lifecycle (phases: 2–6, 8, 10–14 and 16) of submonthly NAM events. The outermost circle in each panel represents the latitude of 20°N .

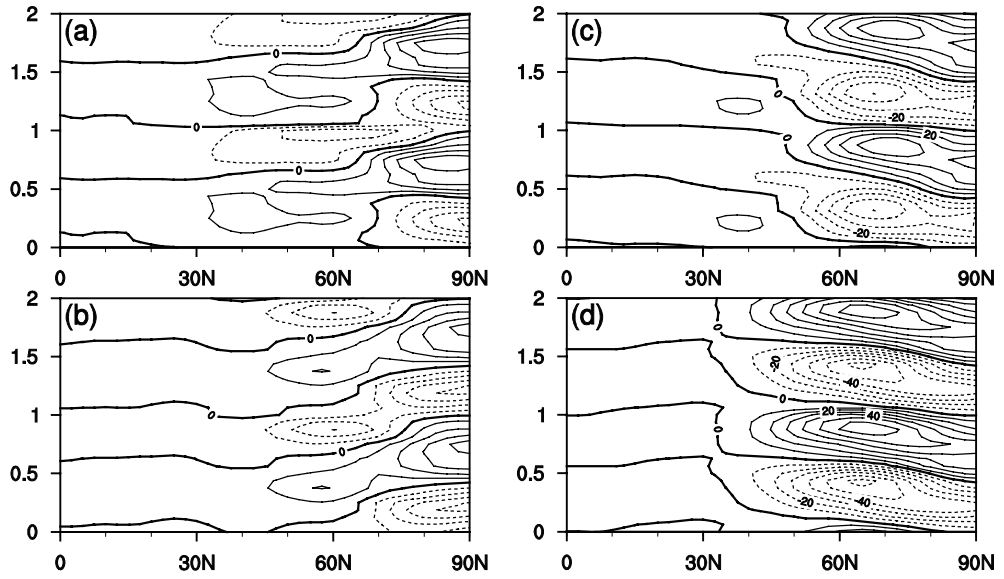


Fig. 10. Zonal-averaged anomalous HGT (units: gpm) over (a) the North American sector (150° – 120° W) and (b) the West Eurasia sector (20° – 80° E), and the zonal-averaged anomaly zonal wind (units: m s^{-1}) over (c) the Atlantic sector (60° W– 0°) and (d) the Eurasia–Pacific sector (90° – 180° E) at 50 hPa as a function of the latitude and lifecycle phase of submonthly NAM events. On the ordinate axis, the number '1' ('2') indicates one (two) complete lifecycle(s) of NAM events, while '0.5' and '1.5' indicate the end of the positive phase, and the start of the negative phase, respectively.

5. Anomalous vertical planetary-scale wave activity

Planetary-scale waves are active along the mid-high latitudes and their variability is closely connected with the NAM (Chen et al., 2003). By expanding the submonthly HGT field into their zonal Fourier harmonics along latitudes, the zonal wavenumbers (WNs) 1–3 can be used to represent the planetary-scale wave activity. Investigating this planetary-scale wave activity may improve our understanding of the submonthly stratosphere–troposphere coupling.

The propagation of tropospheric HGT anomaly over three land areas (North America, Europe, and East Eurasia) is essentially opposite to that over two ocean areas (North Atlantic and North Pacific) during the lifecycle of submonthly NAM events, suggesting the planetary-scale waves with WNs 2 and 3 are dominant in the low troposphere under the context of submonthly NAM variability. As shown in Fig. 11, the upward propagation of anomalous planetary-scale waves from the troposphere to the lower stratosphere can be observed in the middle to high latitudes of the NH in both the positive and negative phases of submonthly NAM events; the upward propagation of these waves is mainly determined by the contributions of zonal waves with WNs 2 and 3 (Figs. 11b and c), especially the zonal waves with WN 2.

When the anomalous planetary-scale waves (mainly WNs 2 and 3) propagate to the low stratosphere from the troposphere, they weaken the anomalous zonal symmetrical flow of the low stratosphere. The variation in the amplitudes of waves with WNs 2 and 3 is anti-correlated with the anomalous zonal-mean HGT field at the 50 hPa level (Fig. 12a), which means that the energy of these waves is transmitted from the low to the upper atmosphere, decreasing the zonally symmetrical flow in the low stratosphere, and forcing it to change towards the opposite phase. With the weakening of the zonally symmetrical flow in the low stratosphere, the anomalous poleward meridional flow is strengthened and the anomalous HGT in the low stratosphere propagates from the high latitudes to the polar region, before propagating downward to the low troposphere, as mentioned above.

After the anomalous HGT propagates downward from the low stratosphere, it moves south over land areas, enhancing the land–sea contrast in the anomalous HGT field. Then, as it increases the amplitudes of the waves with WNs 2 and 3 in the low troposphere along middle latitudes, it forms a feedback loop. The zonally averaged HGT anomalies over land areas, including the North American, European and east Eurasian sectors, propagate south from high latitudes near 70° N to the subtropics near 30° N (Figs. 13d–f). At the same time, the propagation of zonally averaged

HGT anomalies over ocean areas, including the Pacific and Atlantic sectors, is in a northerly direction from the subtropics near 30°N, to the high latitudes near 70°N (Figs. 13b and c), a direction opposite to that over land areas. When the HGT anomalies over land and ocean areas propagate to the middle latitudes from opposite directions, as seen in phases 0–3, 8–11 and 15–16 (Fig. 12b), the difference in the anomalous HGT between the three land areas and two ocean areas along the middle latitudes (40°–60°N) reaches its maximum, inducing an increase in the amplitude of planetary-scale waves with WNs 2 and 3. The above analysis suggests that the submonthly troposphere-stratosphere coupling process can also be considered as a feedback loop of anomalous vertical planetary-scale wave activity.

6. Summary and discussion

This paper has detailed the temporal and spatial evolution of the submonthly annular pattern in ND-JFM circulations using NCEP daily data and a NAMI based on the Zonal Index Paradigm (Li and Wang, 2003). The daily NAMI was used because it performed

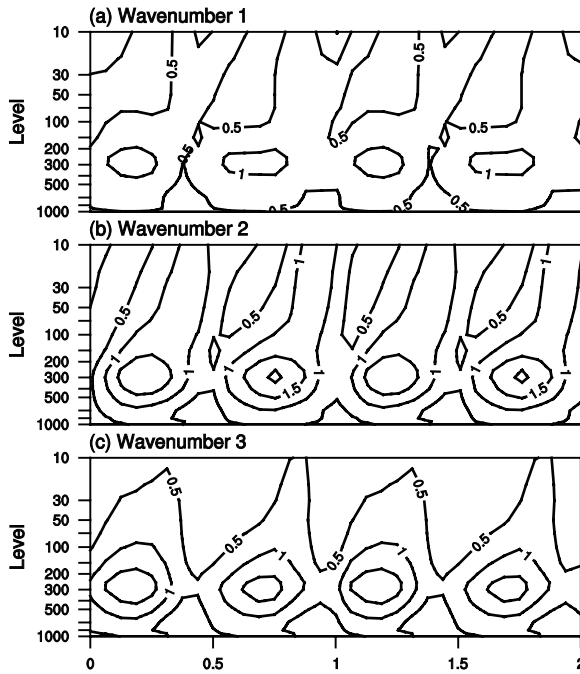


Fig. 11. Evolution of the amplitudes (units: gpm) of planetary-scale waves of (a) WN 1, (b) WN 2 and (c) WN 3 along middle-high latitudes (40°–80°N) associated with the lifecycles of the submonthly NAM events. On the abscissa, the number “1” (“2”) indicates one (two) complete lifecycle(s) of NAM events, while “0.5” and “1.5” indicate the end of the positive phase and the start of the negative phase, respectively.

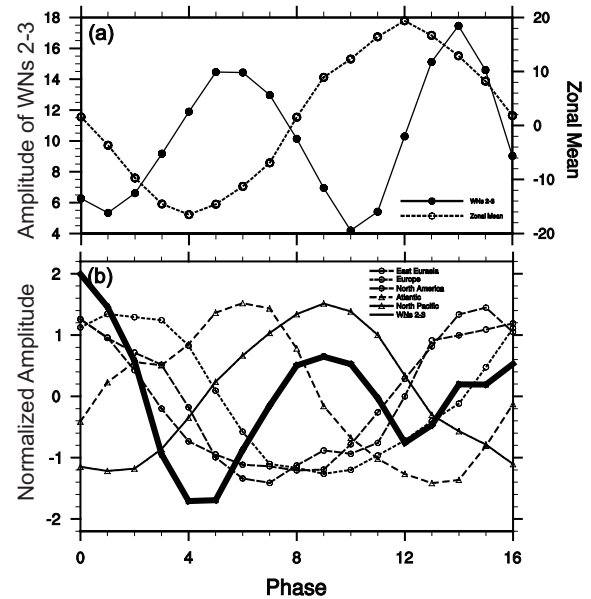


Fig. 12. Evolution of (a) the amplitude (units: gpm) of planetary-scale waves with zonal WNs 2 and 3, and the zonal-averaged anomalous HGT (units: gpm) at 50 hPa level, and (b) the normalized amplitude of planetary-scale waves with zonal WNs 2 and 3 and the normalized zonal-averaged anomalous HGT over the North Pacific sector (180°–140°W), North Atlantic sector (60°–30°W), North American sector (120°–170°W), European sector (0°–60°E), and East Eurasian sector (60°–120°E) along the middle latitudes (40°–60°N) at the 850 hPa level, associated with the life phases of the submonthly NAM events.

well in capturing the zonally symmetrical patterns of atmospheric variability, and it places more emphasis on the connection between the HGT field at middle and high latitudes. As the spectrum of the NAMI in winter has a higher probability of being statistically significant over submonthly periods of around 10 days, we focused on these timescales. This is consistent with the previous study of Feldstein (2000), who suggested that \sim 10 days is the intrinsic timescale of the NAM.

We described a two-way interaction process between the anomalous zonally-symmetrical circulations of the troposphere and the stratosphere within the framework of submonthly NAM events. The tropospheric zonal wind components in the polar regions of the Pacific and Atlantic sectors propagate upwards to the low stratosphere and disturb the polar vortex. The atmospheric mass is then redistributed in the stratosphere, and subsequently propagates downwards, back to the troposphere. From the standpoint of planetary-scale wave activities, anomalous planetary-scale waves with WNs 2 and 3 propagate upwards, disturbing the anomalous zonally symmetrical flow in the low stratosphere, and inducing the anomalous HGT that propa-

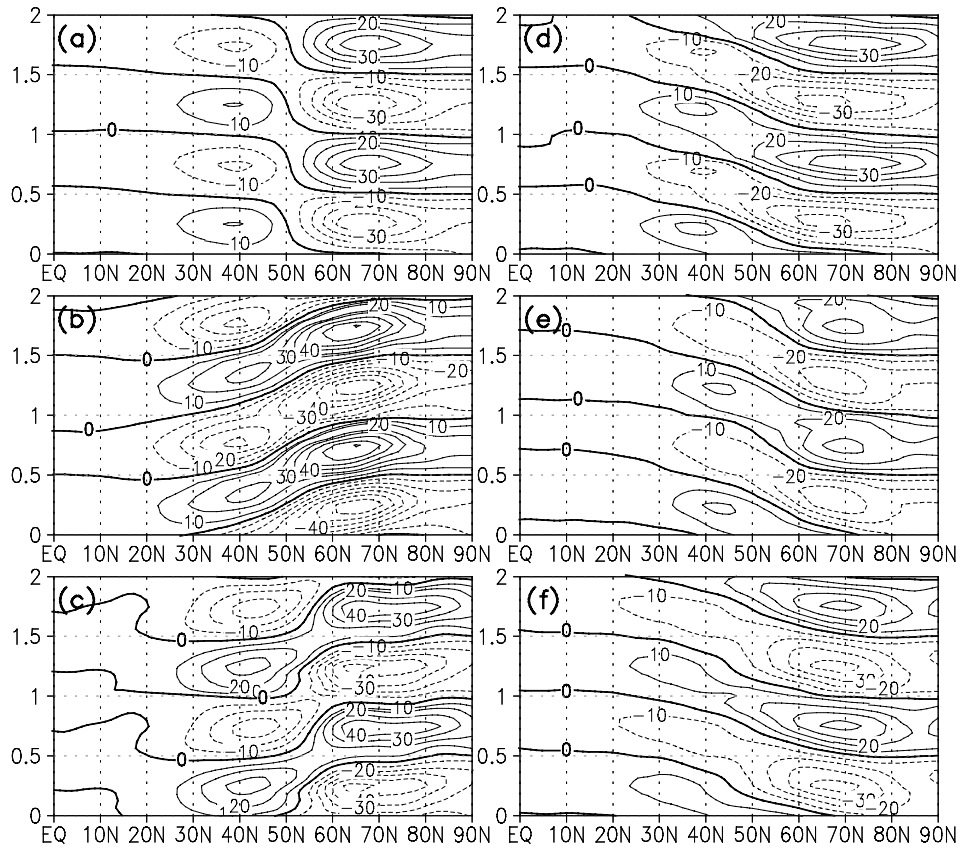


Fig. 13. Zonal-averaged anomalous HGT (units: gpm) at 1000 hPa in the NH (a) between 0 and 357.5° , and over (b) the Pacific sector (180° – 140° W), (c) the Atlantic sector (60° – 30° W), (d) the North American sector (120° – 70° W), (e) the European sector (0° – 60° E), and (f) the east Eurasian sector (60° – 120° E), as a function of the latitude and lifecycle phase of submonthly NAM events. On the ordinate axis, the number '1' ('2') indicates one (two) complete lifecycle(s) of NAM events, while '0.5' and '1.5' indicate the end of the positive phase, and the start of the negative phase, respectively.

gates poleward in the low stratosphere and then down into the troposphere. After the anomalous HGT moves down into the low troposphere, it then travels south over land areas, increasing the energy of waves with WNs 2 and 3 in the low troposphere along middle latitudes by enhancing the land-sea contrast of the anomalous HGT field in the middle latitudes, and forming a feedback loop.

Although symmetrical patterns of atmospheric circulation (e.g. the NAM) are viewed as comprising two phenomena [a tropospheric component at submonthly timescales, and a stratospheric component that persists for a longer period (Thompson et al., 2003)], previous studies (Baldwin and Dunkerton, 1999; Cai and Ren, 2007) place more emphasis on the one-way downward propagation of the stratospheric component, and its influence on the surface climate, because they concentrate on stratospheric fluctuations over longer timescales (1–3 months). However, as ex-

treme NAM values first arise in the upper stratosphere, with no preceding or simultaneous large values in the tropospheric NAM, this gives the misleading impression that the extreme stratospheric events originate in the upper stratosphere (Polvani and Waugh, 2004).

At submonthly timescales, the zonally symmetrical atmospheric circulation shows a clear two-way coupling process between stratospheric and tropospheric components over a single NAM event lifecycle, which provides a detailed new proof to support the viewpoint that the downward propagation of stratospheric NAM signals may not originate in the stratosphere.

In longitudinal circulation, the weather cycles in the Pacific and Atlantic sectors play an important role in the stratosphere–troposphere coupling process. In NDJFM, large low-pressure systems such as the Icelandic Low and the Aleutian Low prevail over the Atlantic and Pacific, respectively, meaning that variations in the atmosphere move readily upwards, with

upward movement near the polar center of the Atlantic and Pacific. Previous studies have also highlighted the importance of atmospheric synoptic activity in these areas (Benedict et al., 2004; Woollings et al., 2008). Local variability, such as the extent of snow cover over Eurasia, has also been shown to modify the stratosphere–troposphere coupling by changing the upward flux of wave activity from the troposphere (Cohen et al., 2007).

Acknowledgements. This study was jointly supported by the R&D Special Fund for Public Welfare Industry (meteorology) of China (Grant No. GYHY201306031), the National Natural Science Foundation of China (Grant No. 40905040) and the National Science Foundation of United States (Grant No. 1107509).

REFERENCES

Angell, J. K., 2006: Changes in the 300-mb north circum-polar vortex. *J. Climate*, **19**(12), 2984–2994.

Baldwin, M. P., and T. J. Dunkerton, 1999: Propagation of the Arctic Oscillation from the stratosphere to the troposphere. *J. Geophys. Res.*, **104**, 30937–30946.

Baldwin, M. P., and T. J. Dunkerton, 2001: Stratospheric harbingers of anomalous weather regimes. *Science*, **294**, 581–584.

Baldwin, M. P., D. W. J. Thompson, E. F. Shuckburgh, W. A. Norton, and N. P. Gillett, 2003a: Weather from the Stratosphere? *Science*, **301**, 317–319.

Baldwin, M. P., D. B. Stephenson, D. W. J. Thompson, T. J. Dunkerton, A. J. Charlton, and A. O'Neill, 2003b: Stratospheric memory and skill of extended-range weather forecasts. *Science*, **301**, 636–640.

Benedict, J. J., S. Lee, and S. B. Feldstein, 2004: Synoptic view of the North Atlantic oscillation. *J. Atmos. Sci.*, **61**, 121–144.

Black, R. X., B. A. McDaniel, and C. Affiliation, 2009: SubMonthly polar vortex variability and stratosphere–troposphere coupling in the Arctic. *J. Climate*, **22**, 5886–5901.

Cai, M., and R. C. Ren, 2006: 40–70 day meridional propagation of global circulation anomalies. *Geophys. Res. Lett.*, **33**, doi: 10.1029/2005GL025024.

Cai, M., and R. C. Ren, 2007: Meridional and downward propagation of atmospheric circulation anomalies. Part I: Northern Hemisphere cold season variability. *J. Atmos. Sci.*, **64**, 1880–1901.

Chen, W., M. Takahashi, and H. F. Graf, 2003: Interannual variations of stationary planetary wave activity in the northern winter troposphere and stratosphere and their relations to NAM and SST. *J. Geophys. Res.*, **108**, doi: 10.1029/2003JD003834.

Cohen, J., M. Barlow, P. J. Kushner, and K. Saito, 2007: Stratosphere–troposphere coupling and links with Eurasian land surface variability. *J. Climate*, **20**, 5335–5343.

Davis, R. E., 1976: Predictability of sea surface temperature and sea level pressure anomalies over the North Pacific Ocean. *J. Phys. Oceanogr.*, **6**, 249–266.

Duchon, C. E., 1979: Lanczos filtering in one and two dimensions. *J. Appl. Meteor.*, **18**, 1016–1022.

Feldstein, S. B., 2000: The timescale, power spectra, and climate noise properties of teleconnection patterns. *J. Climate*, **13**, 4430–4440.

Gao, H., and R. Washington, 2010: Arctic oscillation and the interannual variability of dust missions from the Tarim Basin: A TOMS AI based study. *Climate Dyn.*, **35**(2–3), 511–522.

Kalnay, E., and Coauthors, 1996: The NCEP/NCAR 40-Year Reanalysis Project. *Bull. Amer. Meteor. Soc.*, **77**, 437–471.

Lee, T., T. B. M. J. Ouarda, and J. P. Li, 2012: An orchestrated climate song from the Pacific and Atlantic Oceans and its implication on climatological processes. *Int. J. Climatol.*, doi: 10.1002/joc.3488.

Li, J. P., and J. X. L. Wang, 2003: A modified zonal index and its physical sense. *Geophys. Res. Lett.*, **30**, 1632, doi: 10.1029/2003GL017441.

Li, X. F., and J. P. Li, 2009: Main submonthly timescales of Northern and Southern Hemisphere annual modes. *Chinese J. Atmos. Sci.*, **33**(2), 215–231. (in Chinese)

Li, X. F., and J. P. Li, 2011: Meridional and vertical propagation characteristics of submonthly Northern Hemisphere annual mode. *Acta Meteorologica Sinica*, **69**(6), 1046–1061. (in Chinese)

Polvani, L. M., and D. W. Waugh, 2004: Upward wave activity flux as a precursor to extreme stratospheric events and subsequent anomalous surface weather regimes. *J. Climate*, **17**, 3548–3554.

Rossby, C. G., 1939: Relation between variations in the intensity of the zonal circulation of the atmosphere and the displacements of the semi-permanent centers of action. *Journal of Marine Research*, **2**, 38–55.

Sun, C., and J. P. Li, 2012: Space-time spectral analysis of the Southern Hemisphere daily 500-hPa geopotential height. *Mon. Wea. Rev.*, **140**, 3844–3856..

Thompson, D. W. J., and J. M. Wallace, 1998: The Arctic oscillation signature in the wintertime geopotential height and temperature fields. *Geophys. Res. Lett.*, **25**, 1297–1300.

Thompson, D. W. J., and J. M. Wallace, 2000: Annual modes in the extratropical circulation. Part I: Month-to-month variability. *J. Climate*, **13**, 1000–1016.

Thompson, D. W. J., S. Lee, and M. P. Baldwin, 2003: Atmospheric processes governing the Northern Hemisphere annular mode/North Atlantic oscillation. *The North Atlantic Oscillation: Climatic Significance and Environmental Impact*, J. W. Hurrell, Y. Kushnir, M. Visbeck, and G. Ottersen, Eds., American Geophysical Union, 81–112.

Woollings, T., B. Hoskins, M. Blackburn, and P. Berrißford, 2008: A new Rossby wave-breaking interpretation of the North Atlantic oscillation. *J. Atmos. Sci.*, **65**, 609–626.

Zhang, X., J. E. Walsh, J. Zhang, U. S. Bhatt, and M. Ikeda, 2004: Climatology and interannual variability of Arctic cyclone activity: 1948–2002. *J. Climate*, **17**, 2300–2316.